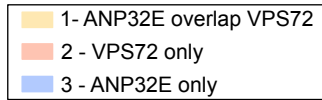
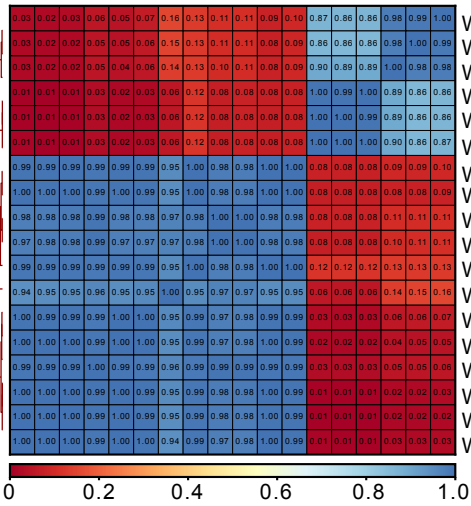
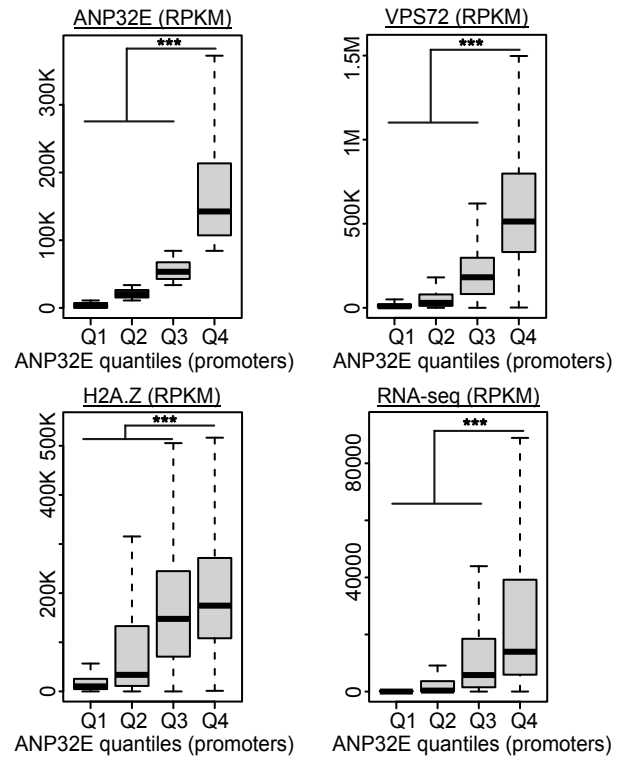
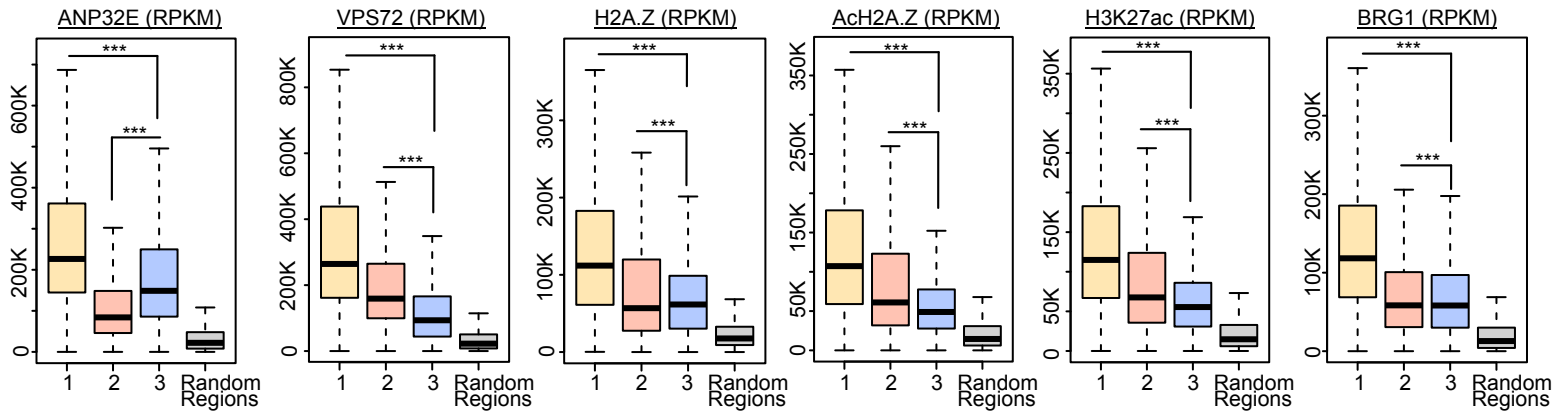
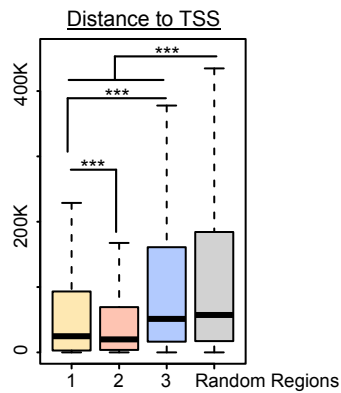


A

Pearson Correlation at promoters

**B****C****D**

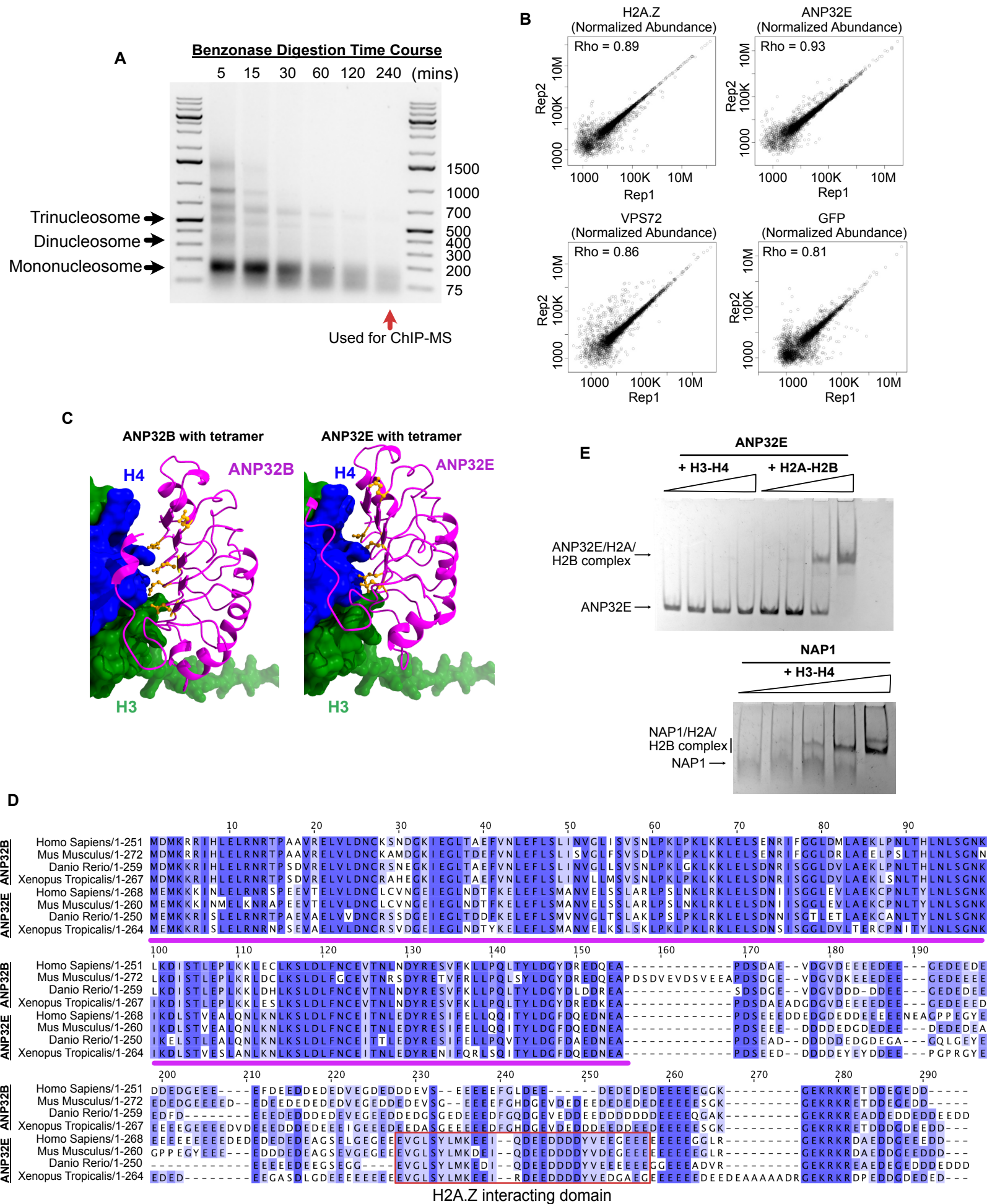
Supplementary Figure 1: The enrichment of ANP32E, VPS72, and H2A.Z are positively correlated with each other

A. Heatmap of Pearson correlation of three replicates for H2A.Z, VPS72, ANP32E, Ach2A.Z, H3K27ac, and BRG1 at promoters in WT MEFs. Pearson correlation values are provided.

B. Boxplots of RPKM enrichment of ANP32E, VPS72, H2A.Z, and RNA-seq across four enrichment quantiles. Quantiles are partitioned based on ANP32E levels at promoters from the lowest signal (Q1) to the highest signal (Q4). One-sided Wilcoxon rank-sum test was used to calculate p-values. ***p < 0.0001.

C. Boxplots of RPKM enrichment of ANP32E, VPS72, H2A.Z, Ach2A.Z, H3K27ac, and BRG1 at the peak regions from the intersection between ANP32E and VPS72 bound loci, and their individual occupied regions. ANP32E only = blue; ANP32E and VPS72 = orange; VPS72 only = pink. One-sided Wilcoxon rank-sum test was used to calculate p-values. ***p < 0.0001.

D. Boxplot of distance from peaks to nearest TSS with regions broken up according to enrichment of ANP32E and/or VPS72. ANP32E only, blue; ANP32E over VPS72, orange; VPS72 only, pink. One-sided Wilcoxon rank-sum test was used to calculate p-values. ***p < 0.0001.



Supplementary Figure 2: The N-terminal of ANP32E is predicated to interact with H3-H4 tetramers as ANP32B

A. Gel electrophoresis of the length of DNA fragments digested by Benzonase at different time points for CHIP-MS. Mononucleosomes = ~150bp fragment length; dinucleosomes = ~300bp fragment length; trinucleosome = ~500bp fragment length.

B. Scatterplot depicts enrichment for two replicates of H2A.Z CHIP-MS, ANP32E CHIP-MS, VPS73 CHIP-MS and GFP CHIP-MS. Positive Rho values indicate a positive correlation between replicates.

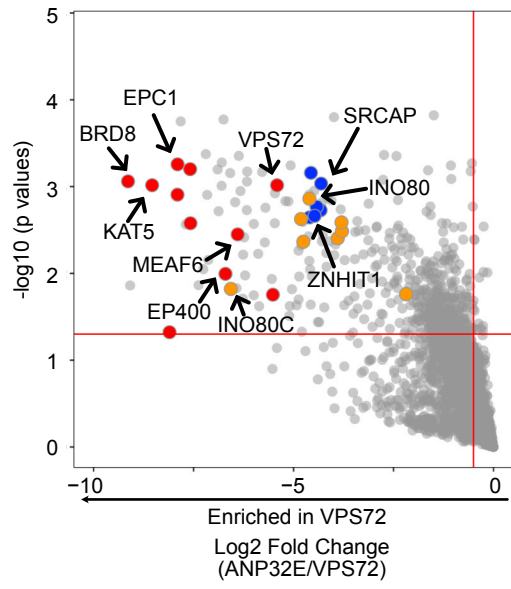
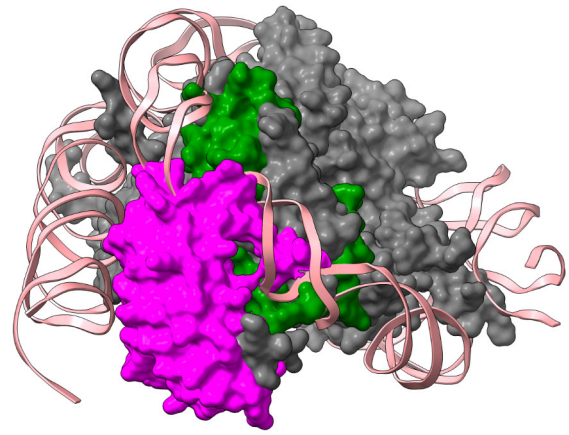
C. AlphaFold3 predicted structure of ANP32B bound with H3-H4 tetramers and ANP32E bound with H3-H4 tetramers. The human protein sequences were used for predictions.

D. Protein alignment of ANP32B and ANP32E in Homo Sapiens, Mus Musculus, Danio Rerio, and Xenopus Tropicalis. The magenta lines highlighted the evolutionarily conserved N-terminal (1-155), and the square highlights the conserved H2A.Z interacting domain (ZID) at the C-terminus of ANP32E.

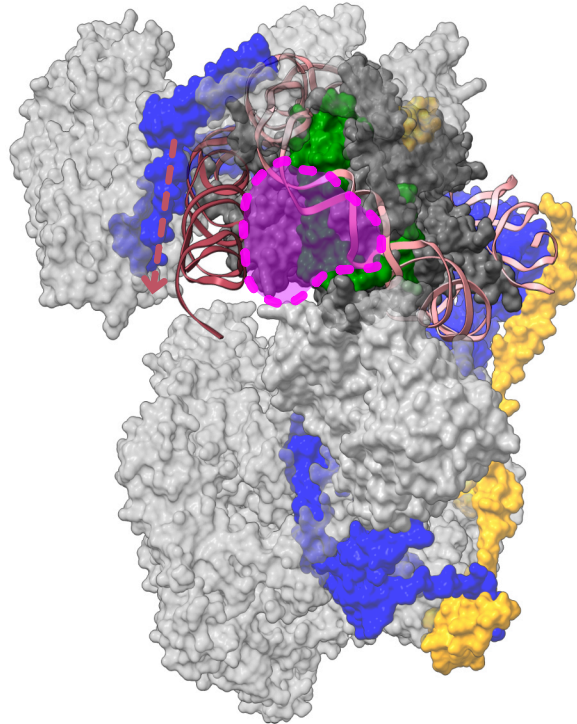
E. EMSA assay investigating the interaction between ANP32E with H3-H4 tetramers or H2-H2B dimers. NAP1 is included a positive control for H3-H4 tetramer interaction.

A

● p400/TIP60 complex ● SRCAP complex ● INO80 complex

**B****C**

■ ANP32E
 ■ H3
 ■ DNA
 ■ SRCAP
 ■ VPS72
 ■ Histone octamer
 ■ All other subunits in SRCAP



Supplementary Figure 3: ANP32E is predicated to interact with histone octamers and stabilizes partial unwrapping nucleosomes within SRCAP complex

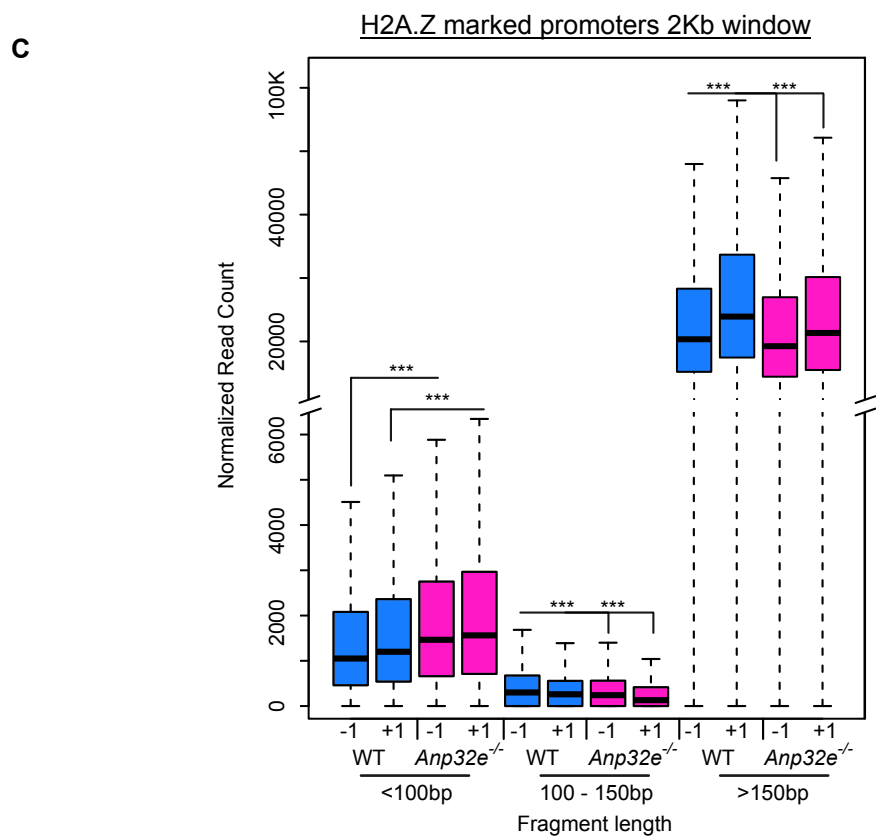
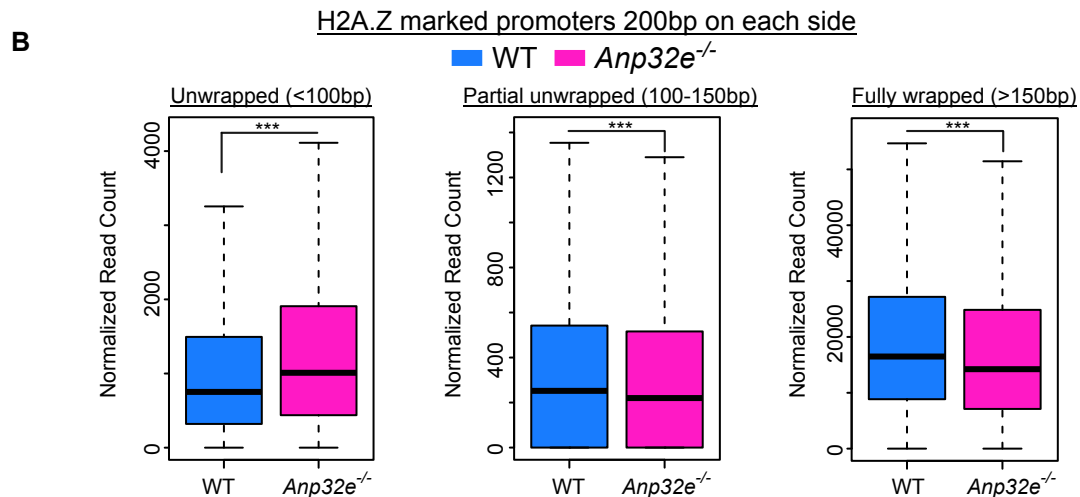
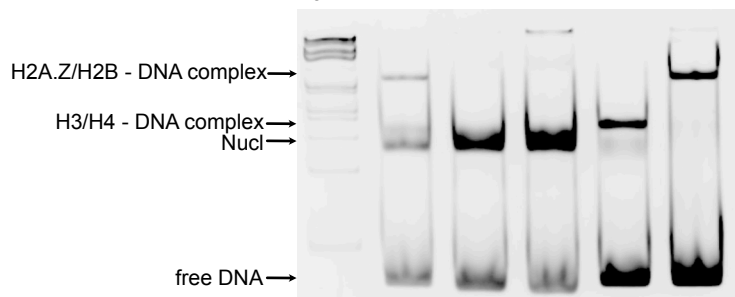
A. Volcano plot of differential interacting proteins comparing the ANP32E CHIP-MS assay against the VPS72 CHIP-MS assay. Only proteins significantly enriched in VPS72 CHIP-MS are shown ($\text{Log}_2\text{FC} < 0.5$ and $p \text{ values} < 0.05$). Major subunits of the p400/TIP60 complex, SRCAP complex, and INO80 complex are labeled in red, blue, and orange, respectively.

B. AlphaFold3 predicted structure of ANP32E bound with partial unwrapped nucleosome. The color of each protein was labeled as follows: H3 - green; ANP32E – magenta.

C. Re-analysis of nucleosome structures when bound by the published active state of the SRCAP remodeling complex, such that AlphaFold3 predicted N-terminal of ANP32E structure has been aligned and overlaid. The transparent magenta dotted lines represent the location where ANP32E binding occurs, based on panel B. DNA is partially unwrapped from nucleosomes when SRCAP is in the active state, and an arrow depicts the location of unwrapped DNA exiting the nucleosome.

A

Lane #	1	2	3	4	5
DNA	+	+	+	+	+
H3/H4 tetramer	+	+	+	+	-
H2A.Z/H2B dimer	+	+	+	-	+
ANP32E	-	+	+++	-	-



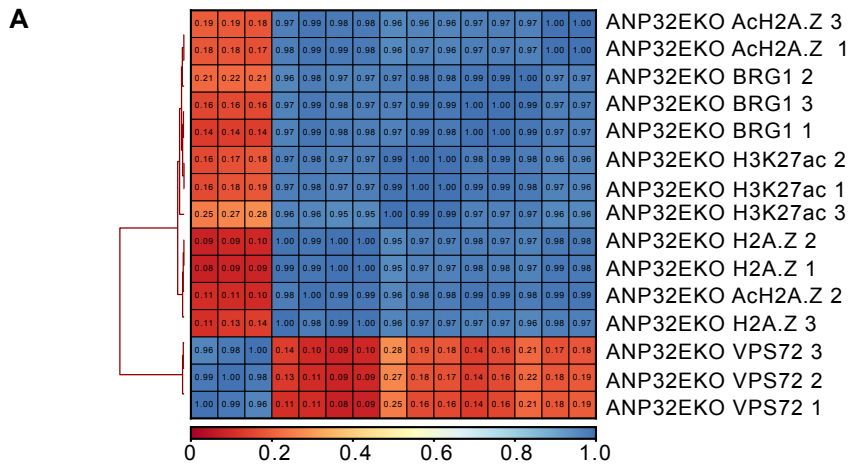
Supplementary Figure 4: Loss of ANP32E caused more unwrapped nucleosomes at downstream of the TSS

A. H2A.Z nucleosome assembly assays in which DNA is incubated with H3/H4 tetramers and H2A.Z/H2B dimers, along with different amounts of ANP32E.

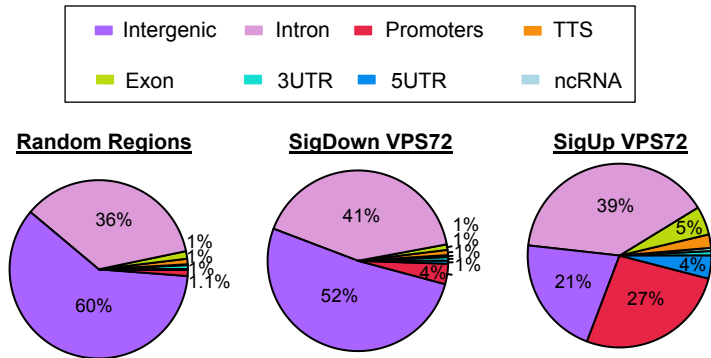
B. Boxplots of normalized read count for DNA fragments wrapped around nucleosomes at H2A.Z-marked promoters (200bp on each side of TSS) in WT and ANP32E null MEFs. Unwrapped = less than 100bp; partial unwrapped = 100 to 150bp; fully wrapped = greater than 150bp. One-sided Wilcoxon rank-sum test was used to calculate p-values. ***p < 0.0001.

C. Boxplots of normalized read count of nucleosome wrapping at downstream (+1 Kb) and upstream (-1 Kb) TSS positions in WT and ANP32E null MEFs. One-sided Wilcoxon rank-sum test was used to calculate p-values and show their significance. ***p < 0.0001.

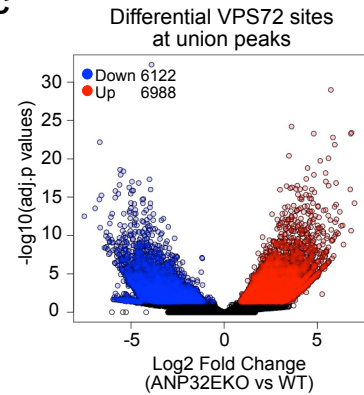
Pearson Correlation at promoters



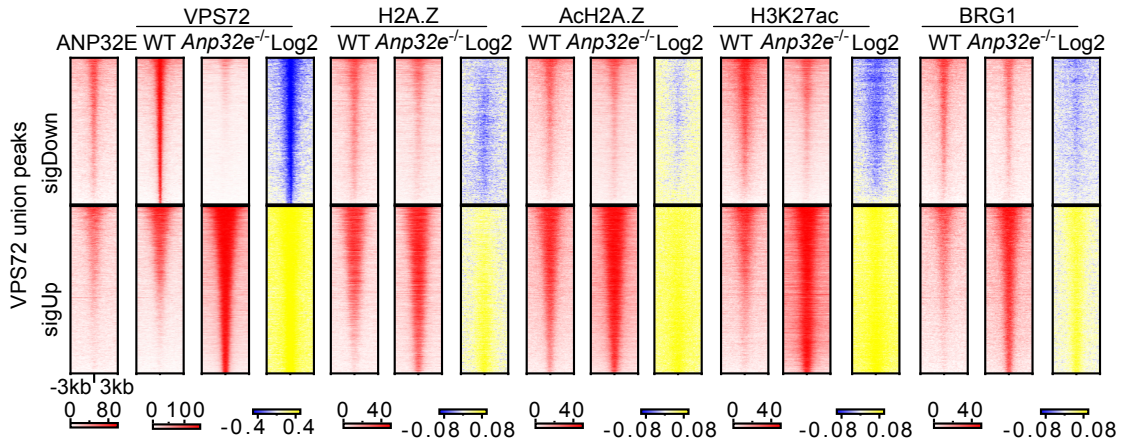
B



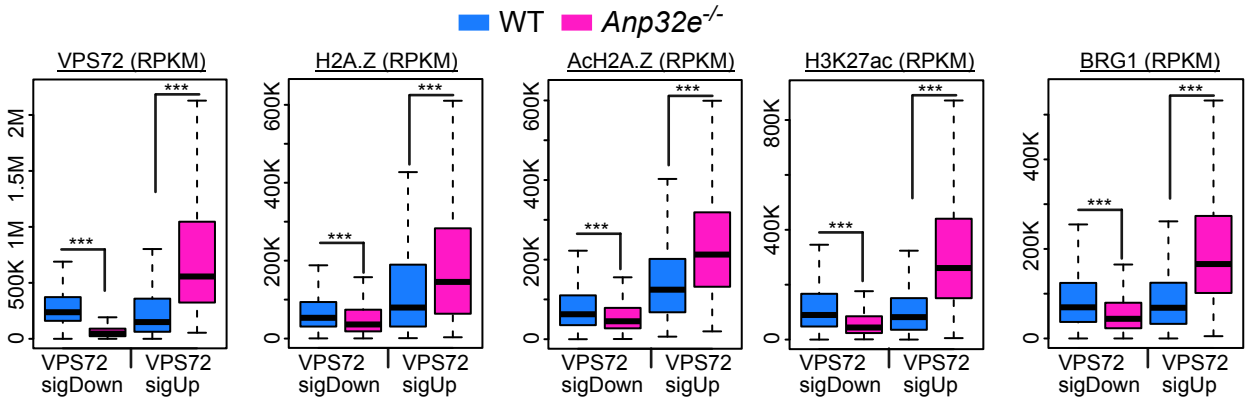
C



D



E



Supplementary Figure 5: Loss of ANP32E led to increased VPS72, H2A.Z, histone acetylation, and BRG1 binding at VPS72 union peaks

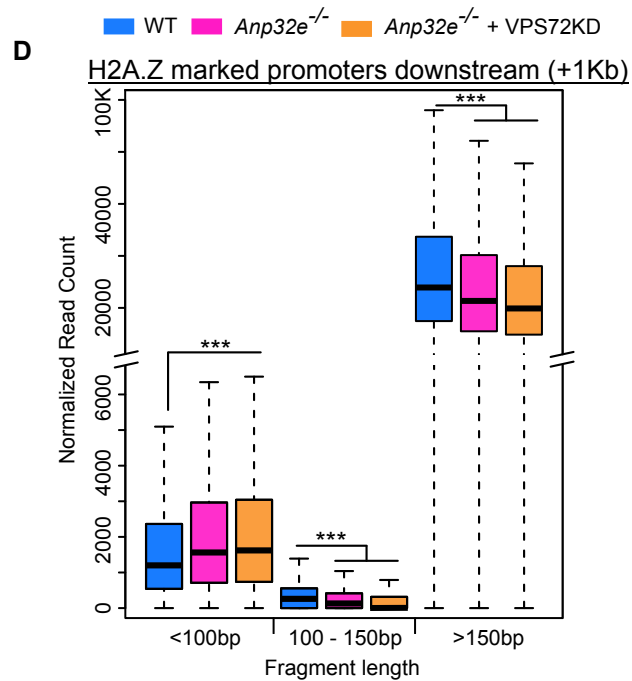
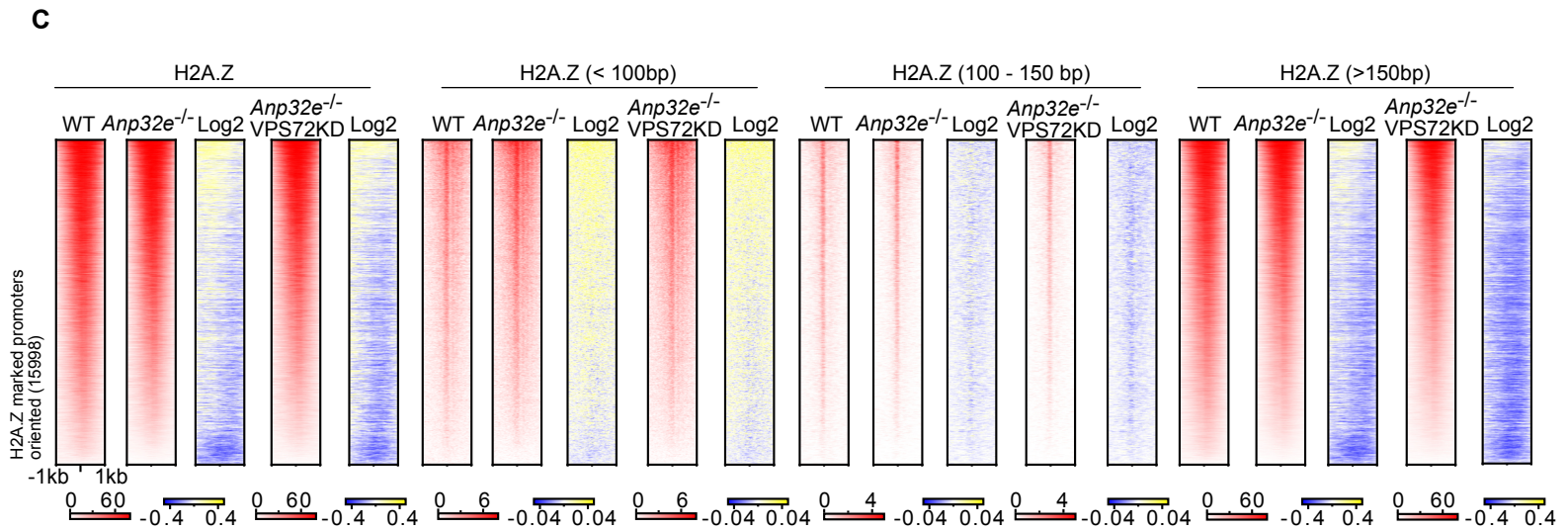
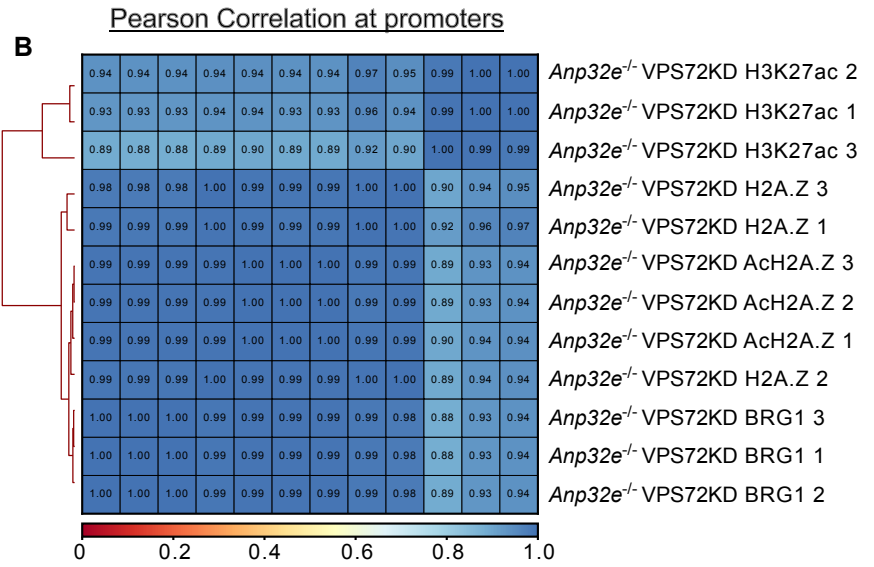
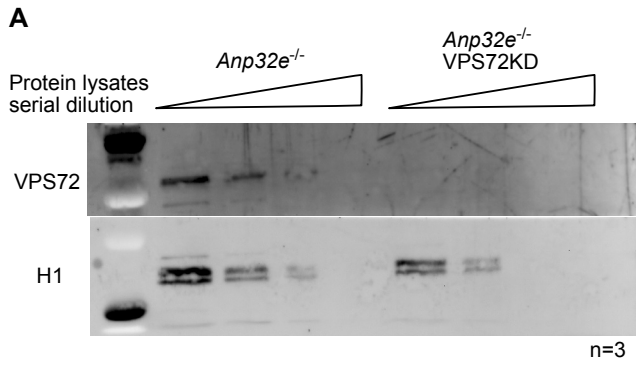
A. Heatmap of Pearson correlations for three replicates for H2A.Z, VPS72, ANP32E, AcH2A.Z, H3K27ac, and BRG1 CUT&Tag at promoters in ANP32E null MEFs. The Pearson correlation values are provided.

B. Pie chart of genomic distribution of increased VPS72 sites and decreased VPS72 sites compared with random regions (55,000 random regions with 250bp fragment length).

C. Volcano plot of differential VPS72 binding in ANP32E null MEFs versus WT MEFs at VPS72 union peaks. Diffbind was used to identify differential binding sites. Increased VPS72 sites (6988 sites) are shown in red ($\log_2FC > 0.5$ and $p. \text{ Adjusted values} < 0.05$). Decreased VPS72 sites (6122 sites) are shown in blue ($\log_2FC < 0.5$ and $p. \text{ Adjusted values} < 0.05$).

D. Heatmap of ANP32E, VPS72, H2A.Z, AcH2A.Z, H3K27ac, and BRG1 enrichment in WT MEFs and ANP32E null MEFs at increased VPS72 sites (peaks) and decreased VPS72 sites (peaks). Log₂ is calculated for the RPKM values in ANP32E null MEFs over WT MEFs.

E. Boxplot of RPKM normalized VPS72, H2A.Z, AcH2A.Z, H3K27ac, and BRG1 enrichment at increased VPS72 sites (peaks) and decreased VPS72 sites (peaks) in WT MEFs and ANP32E null MEFs. WT MEFs = blue; ANP32E null MEFs = magenta. One-sided Wilcoxon rank-sum test was used to calculate p-values. *** $p < 0.0001$.



Supplementary Figure 6: Accumulation of VPS72 in the absence of ANP32E generates hyperaccessible regions at H2A.Z - marked promoters

A. Western blot of VPS72 knockdown in ANP32E null MEFs. ANP32E null MEFs were treated with non-targeting siRNA (left) and VPS72 siRNA (right). Serial dilution of protein lysate concentration (stock, $\frac{1}{2}$, $\frac{1}{4}$, $\frac{1}{8}$) was loaded. The size of the VPS72 protein is 57 kDa, and the H1 control protein is 31 kDa.

B. Heatmap of Pearson correlations for three replicates for H2A.Z, VPS72, ANP32E, AcH2A.Z, H3K27ac, and BRG1 CUT&Tag at promoters in VPS72 knockdown in ANP32E null MEFs. The Pearson correlation values are provided.

C. Heatmap of normalized read count for DNA fragments wrapped around nucleosomes at H2A.Z-marked promoters (TSS \pm 1kb). Unwrapped = less than 100bp; partial unwrapped = 100 to 150bp; fully wrapped = greater than 150bp. For each nucleosome wrapping status, the first log₂ fold change depicts change of ANP32E null MEFs compared with WT MEFs, and the second log₂ fold change depicts change of VPS72 knockdown in ANP32E null MEFs compared with WT MEFs.

D. Boxplot of normalized read count for nucleosome wrapping at loci downstream from TSS (+1 Kb) in WT MEFs, ANP32E null MEFs, and VPS72KD with ANP32E null MEFs. A one- tailed Wilcoxon rank sum test was used to calculate p-values.

***p < 0.0001.